**LA-UR** -82-1769

CONF-830103--15

P

Los Alamos National Laboratory is operated by the University of California for the United States Department of Energy under contract W-7405-ENG-36

LA-UR--82-1769

DE82 016231

TITLE: INVESTIGATION OF RADIAL POWER AND TEMPERATURE EFFECTS IN LARGE-SCALE REFLOOD EXPERIMENTS

AUTHOR(S): Frank Motley



SUBMITTED TO: The large and Small Break LOCA Session of the Second International Topical Meeting on Reactor Thermal-Hydraulics to be held in Santa Barbara, California on January 11-14, 1983.



Los Alamos National Laboratory
Los Alamos, New Mexico 87545

FORM NO 836 R4
ST NO 2629 5/81

# INVESTIGATION OF RADIAL POWER AND TEMPERATURE EFFECTS IN LARGE-SCALE REFLOOD EXPERIMENTS*

Frank Motley
Energy Division
Los Alamos National Laboratory

ABSTRACT

The largest reflood test facility in the world has been designed and constructed by the Japan Atomic Energy Research Institute (JAERI). The experimental test facility, known as the Cylindrical Core Test Facility (CCTF), models a full-height core section and the four primary loops of a Pressurized Water Reactor (PWR). The radial power distribution and temperature distribution were varied during the testing program. The test results indicate that the radial effects, while noticeable, do not appreciably alter the overall quenching behavior of the facility. The Transient Reactor Analysis Code (TRAC) correctly predicted the experimental results of several of the tests. The code results indicate that the core flow pattern adjusts multi-dimensionally to mitigate the effects of increased power or stored energy.

---

## I. INTRODUCTION

The accident analysis codes used for licensing of Pressurized Water Reactors (PWR) consider only the axial behavior within the vessel (one-dimensional analysis). By modeling the most limiting portion (highest power) of the core, it was commonly believed that the code predictions would provide a "conservative" or most limiting prediction of fluid conditions or rod temperatures. The heat transfer and core flooding correlations used in these one-dimensional codes were based on data from small-scale test facilities that behave in a uniform manner.

*Work performed under the auspices of the United States Nuclear Regulatory Commission.

The Los Alamos National Laboratory is developing a best-estimate systems code known as the Transient Reactor Analysis Code (TRAC) for analyzing PWR accidents .[1] The code has two-phase nonequilibrium hydrodynamics models, flow-regime-dependent constitutive equation treatment, and reflood tracking capability for both bottom flood and falling-film quench fronts. The entire accident sequence can be followed beginning with steady-state normal operating conditions and then proceeding through the blowdown, refill, and reflood phases of the accident. A full three-dimensional flow calculation can be done within the reactor vessel. This allows an accurate calculation of the complex multidimensional flow patterns inside the reactor vessel that determine the core behavior during the accident. As a best-estimate code, TRAC can help identify excessively conservative or non-conservative assumptions currently mandated for reactor accident design.

The TRAC is verified by comparison of code predictions with many different experiments investigating different aspects of the postulated accident sequence. The most extensive model of a PWR is the Cylindrical Core Test Facility (CCTF),[2] which was constructed by the Japan Atomic Energy Research Institute (JAERI) as part of a tri-lateral agreement among the United States (US), Germany (FRG), and Japan named the 2D/3D Project. The test facility is a model of a 1000 MW PWR. It can simulate the end of blowdown and the refill and reflood phases of a postulated accident. The core of this test facility is large enough to investigate multidimensional effects. A special series of two tests were performed to investigate multidimensional effects. One was a skewed power test [C1-17 (Run 36)] and another was a skewed-initial-temperature test [C1-20 (Run 39)]. These tests are compared with the Base Case test [C1-5(Run 14)] which had a moderate radial peaking and the Evaluation Model (EM) test [C1-19(Run 38)] which had a more peaked radial distribution. Some results of the TRAC analysis of these experiments are presented to explain the observed experimental behavior.

## II. DESCRIPTION OF CCTF FACILITY AND TRAC MODEL

The test facility is a model of a four-loop PWR. The experimental core consists of 1824 electrically heated rods contained in a vessel that models the downcomer, lower plenum, and upper plenum. There are three intact loops and a fourth loop with a cold-leg break. Each loop contains an active steam

generator and a passive pump simulator. The facility is full height and scaled in volume by the ratio of the number of heated rods (1824/39372), roughly a 1/20 factor.

The TRAC input model attempts to reproduce all the pertinent details of the facility's geometry. The overall CCTF facility model is shown in Fig. 1. Only one of the intact loops is shown because all the intact loops are modeled identically. All the hot legs (connecting the upper plenum and the steam generator) are identical. Each loop contains an active steam generator. The secondary sides of the steam generator are isolated. The remainder of the intact loop piping (connecting the steam generator to the downcomer) is modeled, including the loop seal, pump simulator, and emergency core coolant (ECC) injection. The pump simulator has an orifice to represent the resistance of an impeller. This orifice is modeled in TRAC as additional friction. The ECC injection enters through the secondary-side branch of a tee between the pump simulator and the vessel. In the TRAC model, ECC liquid is supplied to this pipe in the same manner as in the experimental facility. This is discussed further in the boundary conditions section. The broken-loop model is identical to the intact-loop model from the steam generator to one cell following the pump simulator. There is no ECC injection in this loop and, instead of connecting to the downcomer, the end of the component is connnected to a pressure boundary similar to that provided by the containment tank in the facility. The other portion of the broken loop is modeled by a pipe extending from the vessel to the same pressure boundary as the other end of the broken cold leg. Initially, ECC water is delivered to the lower plenum. The boundary conditions at this location will be discussed in a later section.

The overall vessel noding is shown in Fig. 2. The inner three rings represent the core. The inner radial ring (cells 1 through 4) corresponds to the inner power zone. The remaining power zones each correspond to a single TRAC cell. The outer-most radial ring in the TRAC noding corresponds to the downcomer and the barrel-baffle region. The vessel is divided axially into sixteen levels. The downcomer extends from the top of the first level to the top of the vessel. The lower plenum is contained in the bottom three levels.

The heated core extends from 2.1 m to 5.76 m. It is divided axially into seven segments. The volume fractions and flow areas at each of the elevations are equal to those of the rod matrix. The remaining vessel levels were chosen to maintain the proper elevation of the loop connections. The top of the fourteenth level corresponds to the bottom of the loop pipes, which allows proper modeling of the downcomer height. The loops are connected at the fifteenth level, with the cold-leg connection into the outer downcomer ring and the hot-leg connection into the upper plenum at the third radial ring. One loop is connected to each azimuthal section. Because there is a composite of different upper plenum hardware in each of the upper plenum cells, averaged flow areas and volume fractions are used. The lower plenum injection connection is at the outer ring of the first level. All stored energy associated with the pressure vessel walls, core barrel assembly, upper and lower plenum internals, and non-heated rods in the core region was modeled.

The 1.49 peak-to-average chopped-cosine axial power profile is divided into the seven axial core levels. The power distribution is modeled by the twelve nodes on each level. The radial power profile of the Base Case and the skewed-initial-temperature test was 1.15 in the inner ring, 1.08 in the intermediate ring, and 0.89 in the outer ring. The EM test peaked more radially, with 1.30 for the inner ring, 1.09 for the intermediate ring, and 0.84 for the outer ring. The skewed-power-test had 1.15 in the inner ring but the outer two rings were split into a hot and cold side. The intermediate ring had 1.17 on the hot side and 1.03 on the cold side. The outer ring had 0.91 on the hot side and 0.87 on the cold side.

## III. INITIAL AND BOUNDARY CONDITIONS

The TRAC calculation was similar to the execution of the test. Starting from an initial condition, there was a constant power heatup period. When some of the rod locations attained a predetermined temperature, ECC injection was initiated into the lower plenum from an accumulator and continued until shortly after water began to penetrate the core. A power decay was initiated at the beginning of core recovery (BOCREC). The ECC injection was switched from the lower plenum to the cold legs, and then switched from accumulator

injection to a low-pressure coolant injection (LPCI) equivalent flow rate shortly after BOCREC. This lower ECC injection flow continued until all the rods were quenched. The skewed temperature test had an initial core temperature distribution which was skewed up to 350 K along a core diagonal, hot rods in the lower half to cold rods in the upper half in Fig. 2. This distribution was obtained by pulsing the power selectively to the various heater regions before starting of the test.

## IV. EXPERIMENTAL AND TRAC CALCULATION RESULTS

This section is divided into two parts. First the experimental results will be presented and then the TRAC calculation results will be compared with the experiment.

### A. Experimental Results

Some of the pertinent results of the four experiments are compared in Table 1. The initial conditions for each of the tests were intended to be the same with the exception of the EM test, which had a longer heating period before bottom of the core recovery (BOCREC). This extended heatup period resulted in 60% more stored energy in the core. The skewed initial temperature test had a shorter heating period before BOCREC but the stored energy in the core was similar to the Base Case and skewed-power test because of the preheating of part of the core to establish the 350 K skewed temperature distribution.

The EM and skewed-initial-temperature tests show earlier turnaround of the high temperature rods than does the Base Case or the skewed-power test. The final turnaround occurred latest on the cooler rods of the skewed-initial-temperature test and on the low powered rods of the skewed-power test. The EM test has a slightly earlier final turnaround than the Base Case test, but the difference is insignificant.

The final quench time of all the rods only varies by 40 s among all the experiments. The similarity of quench behavior of all the runs is illustrated by Fig. 3, which shows the quench time versus elevation for one of the central

bundles. This bundle contains the highest power and temperature rods. There is only a 40 s variance in quench times at each elevation. This is within the experimentally observed variance of quench times of equally powered rods in one assembly of one test so this variation between experiments is insignificant.

The quench behavior of two bundles on opposite sides of the intermediate heating zone is shown in Figs. 4 and 5. Bundles on opposite sides were chosen to correspond to the hot or high-powered side (Fig. 4) and the cooler or low powered side (Fig. 5) for the skewed-initial-temperature and skewed-power tests. The effect of skewing the power or initial temperature is most noticeable in the bottom two levels of the core (0.38 m and 1.01 m). As expected the cooler or low powered side of the core quenches more rapidly than the base case and the hot or higher powered side quenches more slowly. But at the midplane elevation (1.83 m), the differences between the experiments has become insignificant. The skewed-initial-temperature test has a slightly delayed quench at the top portion of the core, but the delay is the same on both the hot and cooler sides of the core.

The temperature response of the rods in two opposite core segments along the temperature skew direction is shown in Figs. 6 and 7. Comparison of the two shows that before water enters the core, the rods heat at a similar rate, maintaining the initial temperature skew. When the water begins flooding the bottom of the core, the bottom sixth of the cooler rod (Fig. 7), which is below the minimum film boiling temperature, quenches immediately. At the same elevation the hotter rod (Fig. 6) begins cooling, but quenching is delayed 50 s while the rod cools to the minimum film boiling temperature. At the next core level (Z = 1.01 m) the temperature turnaround time is identical on both sides of the core, but because the hotter side is 250 K higher, quenching is delayed by 45 s. The cooling rate of the hotter rod is greater than that of the cooler rod. The temperature response of the midplane and above elevations is similar. The hotter rod temperatures do not increase after core flooding begins, whereas the cooler rods continue heating. The peak clad temperatures at these levels are only 100 K different (whereas initial temperatures were 350 K different). The quench times are identical for both rods at midplane and above elevations.

This behavior is caused by the water level that is the same on both sides of the core. In the lower part of the core the water level determines quenching. In the upper part the quenching is determined by steam flow and entrainment. On the hotter side of the core the steam flow is increased because of the greater heat input due to the higher initial rod temperature. A similar situation exists in the skewed-power test. In the EM test the high peaking in the center of the core did not delay the quench; so it is likely that the greater power input provided better cooling.

Figure 8 compares the integrated core water delivery among the experiments. This was calculated by summing the water input to the test facility and then subtracting the liquid discharged from the broken cold leg. The water produced by the condensation from the subcooling of the input water was also accounted for. There is no appreciable difference in flooding in any of the experiments except for the first few seconds of the EM test, when the filling was more rapid. It is impossible to say whether this rapid filling is a result of the higher water input or higher initial energy of this test.

## B. TRAC Calculation Results

TRAC version PD2 was used to analyze these experiments, except for the skewed-power test, which was not analyzed with the code because of its similarity to the skewed-initial-temperature test. The code's predictive capability is demonstrated by the excellent agreement between the experimental data and the code predictions presented in a previous paper.[3] As an example of the agreement the measured and predicted rod temperatures for several bundles from different tests are presented. Figure 9 shows a central high power rod in the EM test. The TRAC predicted temperatures are included on Figs. 6 and 7, which showed the temperature responses of two rods from the skewed-initial-temperature test. In both tests there is good agreement between the experiment and the code predictions.

An extensive investigation of the TRAC results was made to explain the quenching behavior observed in the experiments and predicted properly by TRAC. The results indicate that radial power or temperature differences are

self-mitigating such that the overall core cooling was similar for all the experiments. The three-dimensional analysis capability of TRAC shows that this is accomplished by adjustment of the flooding such that the higher-powered or higher-temperature locations in the core receive more flow. To illustrate this, the axial and radial liquid velocities in the bottom half of the core are shown schematically in Figs. 10 and 11 for the EM test (Run 38) and in Figs. 12 and 13 for the skewed initial temperature test (Run 39). The figures represent a vertical slice through the bottom half of the core. In the case of the skewed-initial-temperature test, the slice is in the same direction as the initial temperature skew. In both tests the times chosen correspond to the filling of levels 6 and 7. The velocity vectors are scaled to the nominal whole core flooding rate (the slope of Fig. 8) which is consistent with the core flow area. At the 2.1 m elevation, the flow area is reduced by 50% to represent the flow area through the grid plate at the bottom of the core.

In the EM test (Fig. 10) a symmetrical circulation pattern is set up in the core. Liquid flows up in the high-powered central assemblies then out radially at the quenching level. The liquid then drains to the bottom of the core through the lower-powered pheripheral assemblies. It then flows radially into the center to begin the cycle again. This circulation pattern persists as the core fills. The core inlet flow is affected by the circulation pattern within the core such that there is more flow into the central high-power assemblies than into the pheripheral low-powered assemblies.

The initial temperature skew of Run 39 influences the circulation pattern early in the transient. In Fig. 12 the upward axial flows on the hot side of the core are accentuated, as is the downward flow on the cold side of the core. This skewing also is evident in the core inlet flows. Later in the transient (Fig. 13), the influence of the initial temperature skew has disappeared and a symmetrical circulation pattern is established. This behavior is consistent with the observed and calculated rod quenching behavior.

The three-dimensional analysis capability of TRAC has allowed the correct prediction of the multidimensional reflood characteristics observed in these

experiments. The code indicates that the core flow pattern is determined by the radial power distribution and that the initial conditions before core reflood only influence the flow pattern briefly. Similar core flooding behavior was calculated for another large-scale test facility, the Slab Core Test Facility (SCTF).[4] The multidimensional hydraulic effects alleviated the effect of a skewed power distribution by adjusting the flow velocities in accordance with the radial power distribution.

## V. CONCLUSIONS

The experimental results from the CCTF large-scale test facility indicate that the core reflood and quenching behavior is very similar for a group of tests with varied power distributions and initial temperature distributions. Locations having increased power or temperature have earlier turnaround of the clad temperature and do not have a delay in quenching. The three-dimensional analysis capability of TRAC enables it to predict correctly the behavior of these experiments. The code results indicate that the core flooding adjusts to mitigate the effects of increased power or stored energy. The implication of these results is that for PWR accident analysis the radial peaking will not significantly affect the core flooding rate or the final quenching.

REFERENCES

1. "TRAC-PD2: An Advanced Best-Estimate Computer Program for Pressurized Water Reactor Loss-of-Coolant Accident Analysis," Los Alamos National Laboratory report LA-8709-MS (May 1981).

2. Test conditions and data supplied through personal communications from Dr. Hirano (JAERI) to Los Alamos National Laboratory.

3. F. Motley, "Verification of the Three-Dimensional Thermal-Hydraulic Models of the TRAC Accident Analysis Code," Proceedings of Kiamesha Lake Meeting on Advances in Reactor Physics and Core Thermal Hydraulics, September 1982.

4. R. Fujita, "TRAC Analysis of Radial Power Distribution Effects on Force-Feed Reflood Experiments," Proceeding of Second International Topical Meeting on Nuclear Reactor Thermal Hydraulics, January 1983.

TABLE I

| Parameter | Base Case C1-5 Run 14 | Skewed Power C1-17 Run 36 | Evaluation Model C1-19 Run 38 | Skewed Initial Temperature C1-20 Run 39 |
|---|---|---|---|---|
| Initial rod temperature | saturation | saturation | saturation | skewed by 350 K |
| Initial rod power | 9.36 MW | 9.4 MW | 9.28 MW | 9.4 MW |
| BOCREC | 63 s | 63.5 s | 102 s | 31 s |
| Turnaround of hot rod temperature (32-3) | 74 s | 70.5 s | 36 s | 61.5 s |
| Turnaround temperature | 997 K | 1005.3 K | 1173.5 K | 1219.2 K |
| Final turnaround | 184.5 s | 212 s | 172.5 s | 233.5 s |
| Final quench | 535 s | 497.5 s | 513 s | 577.5 s |

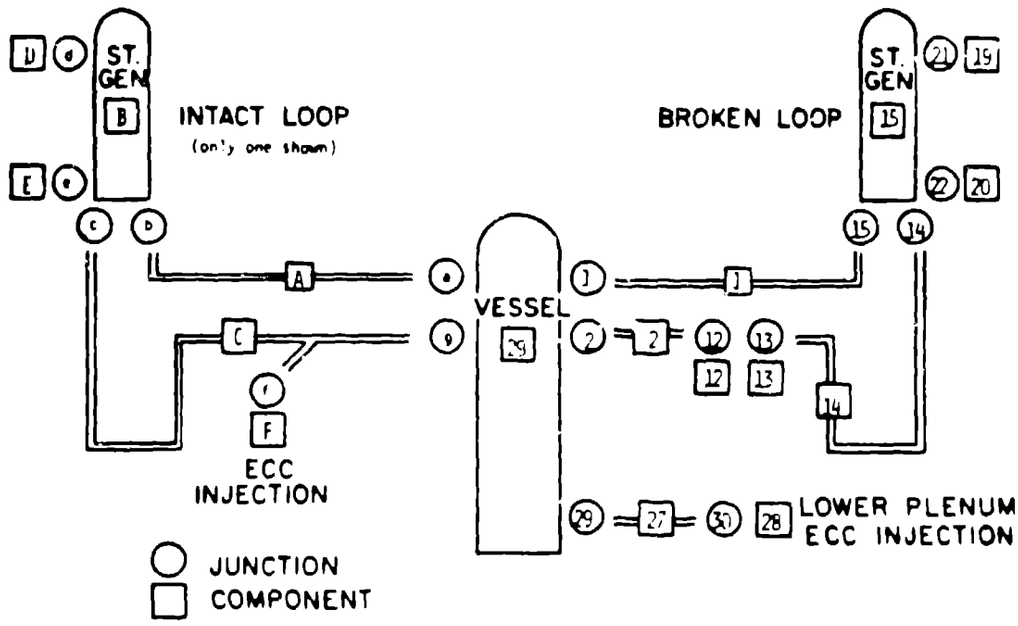


Fig. 1. Schematic of Cylindrical Core Test Facility.

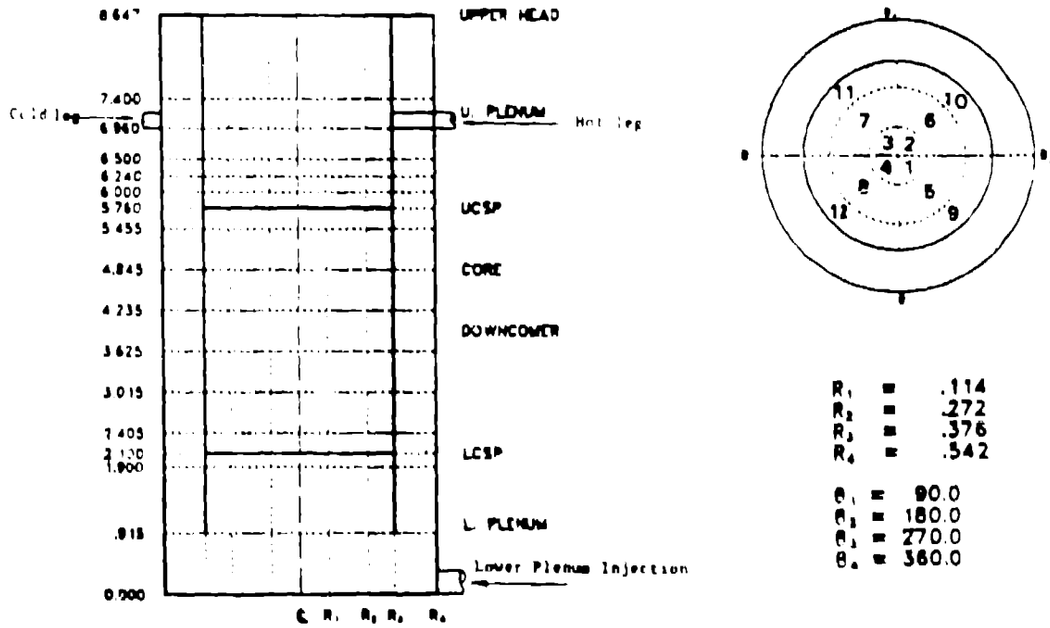


Fig. 2. TRAC noding for the CCTF vessel.

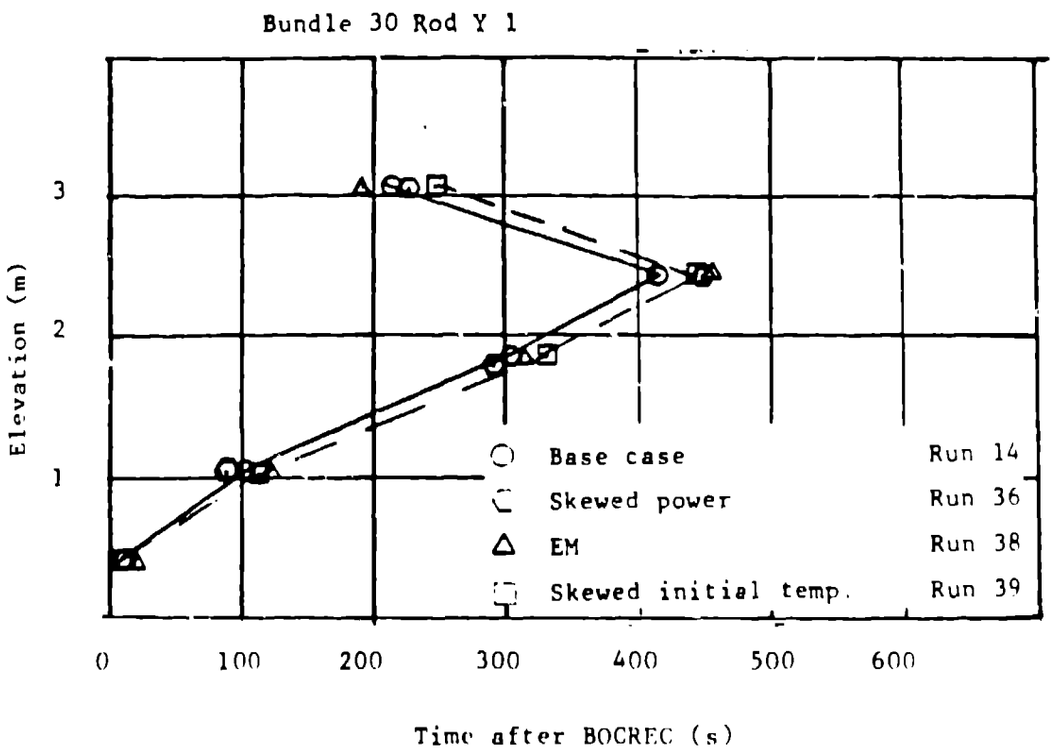


Fig. 3. Quench envelopes for hottest bundle.

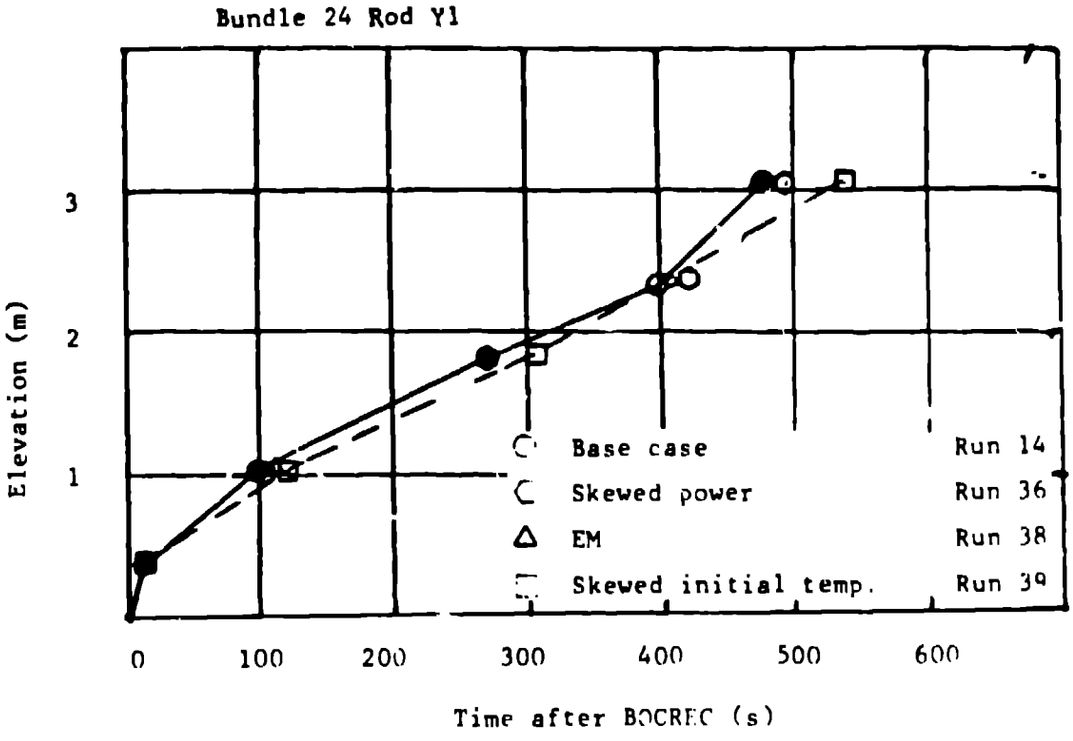


Fig. 4. Quench envelopes for a bundle on the hot or high – powered side of the core.

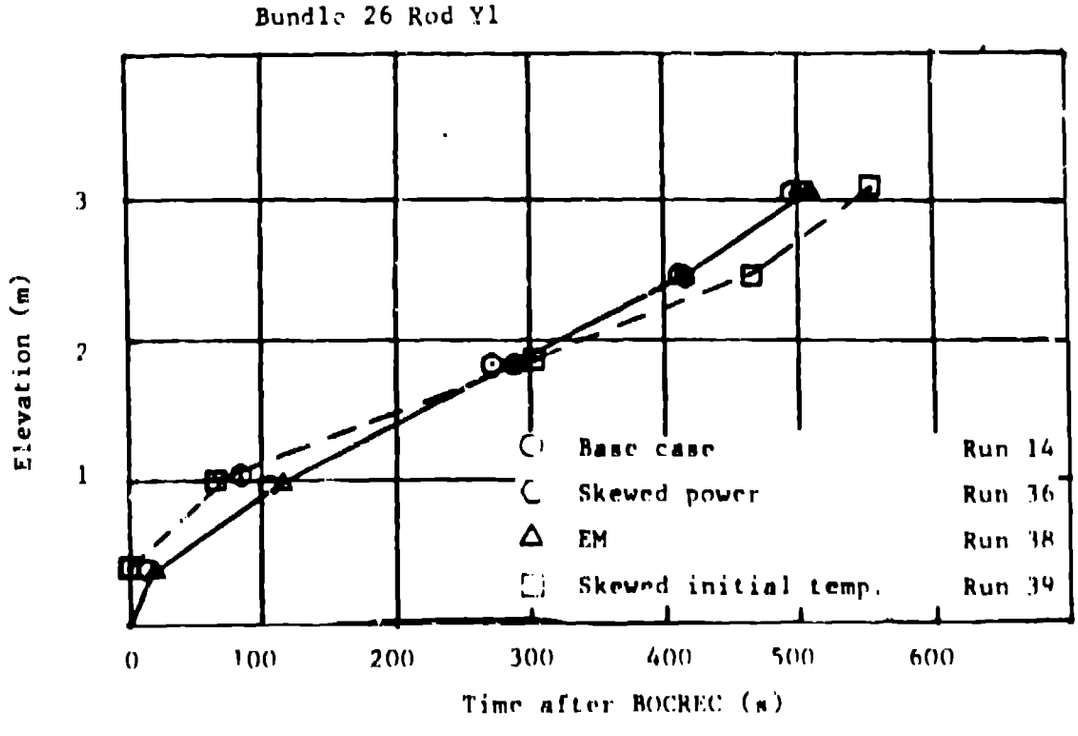


Fig. 5. Quench envelopes for a bundle on the cooler or low-powered side of the core.

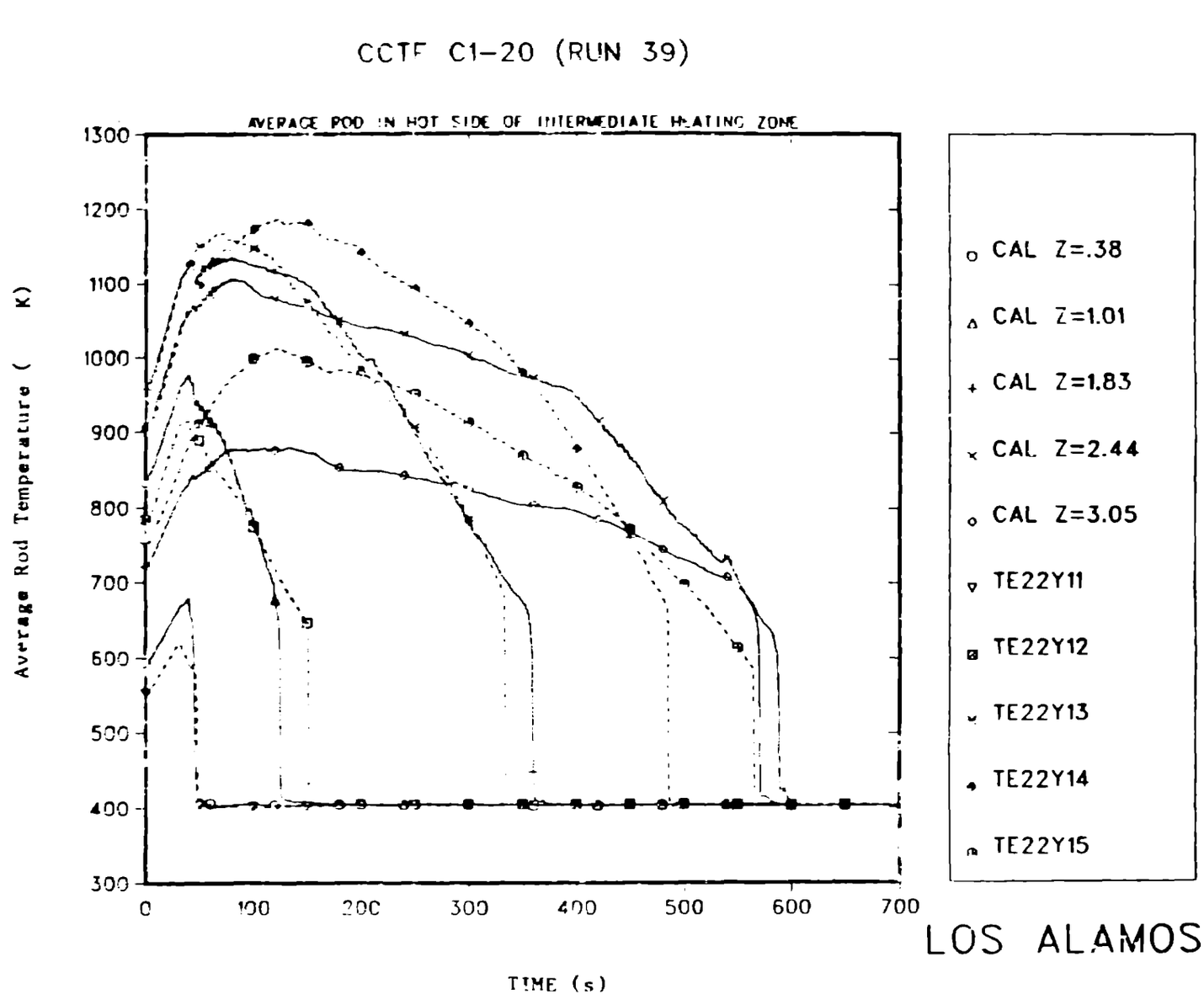


Fig. 6. Temperature response of a rod on the hotter side of the core.

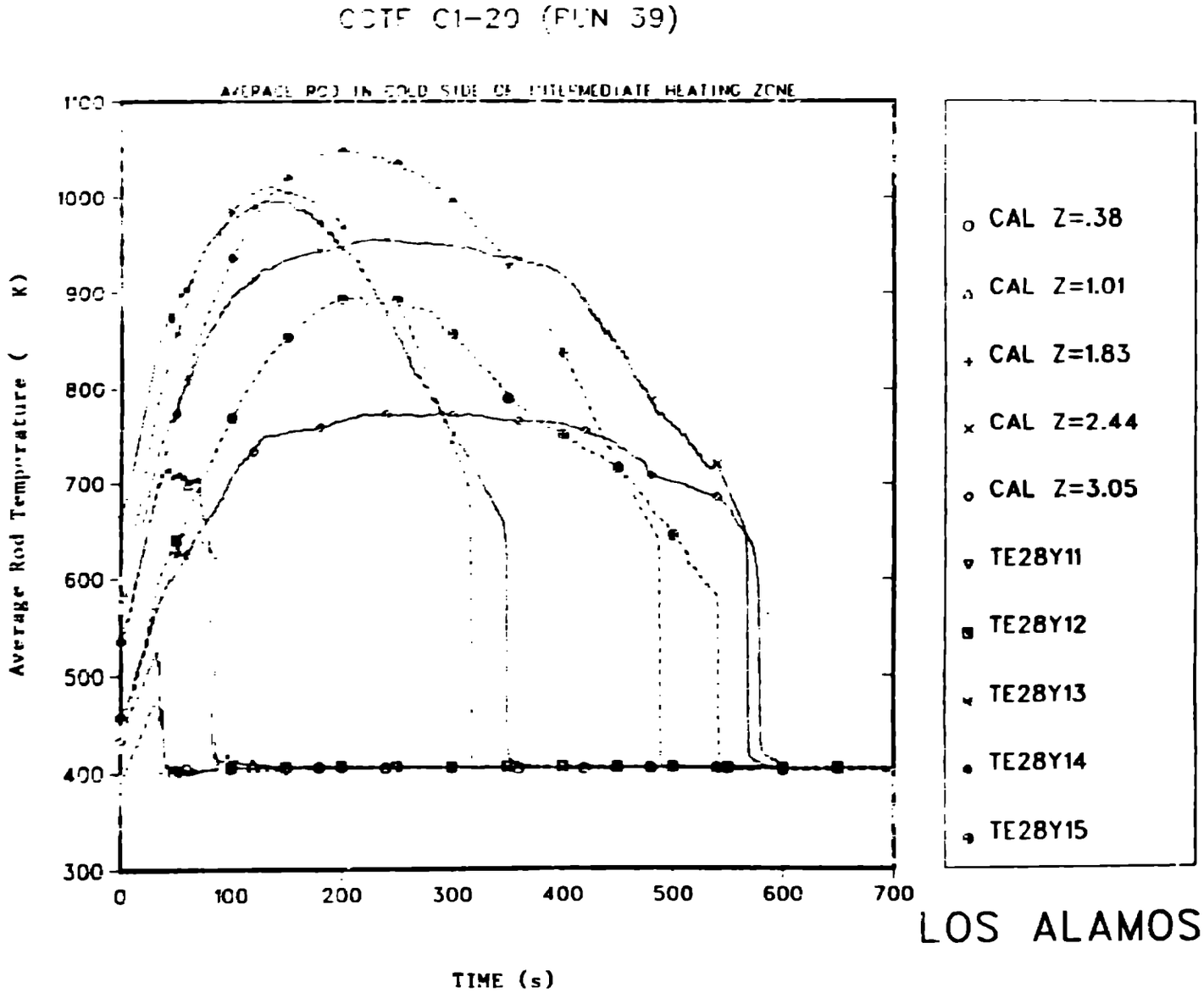


Fig. 7. Temperature response of a rod on the cooler side of the core.

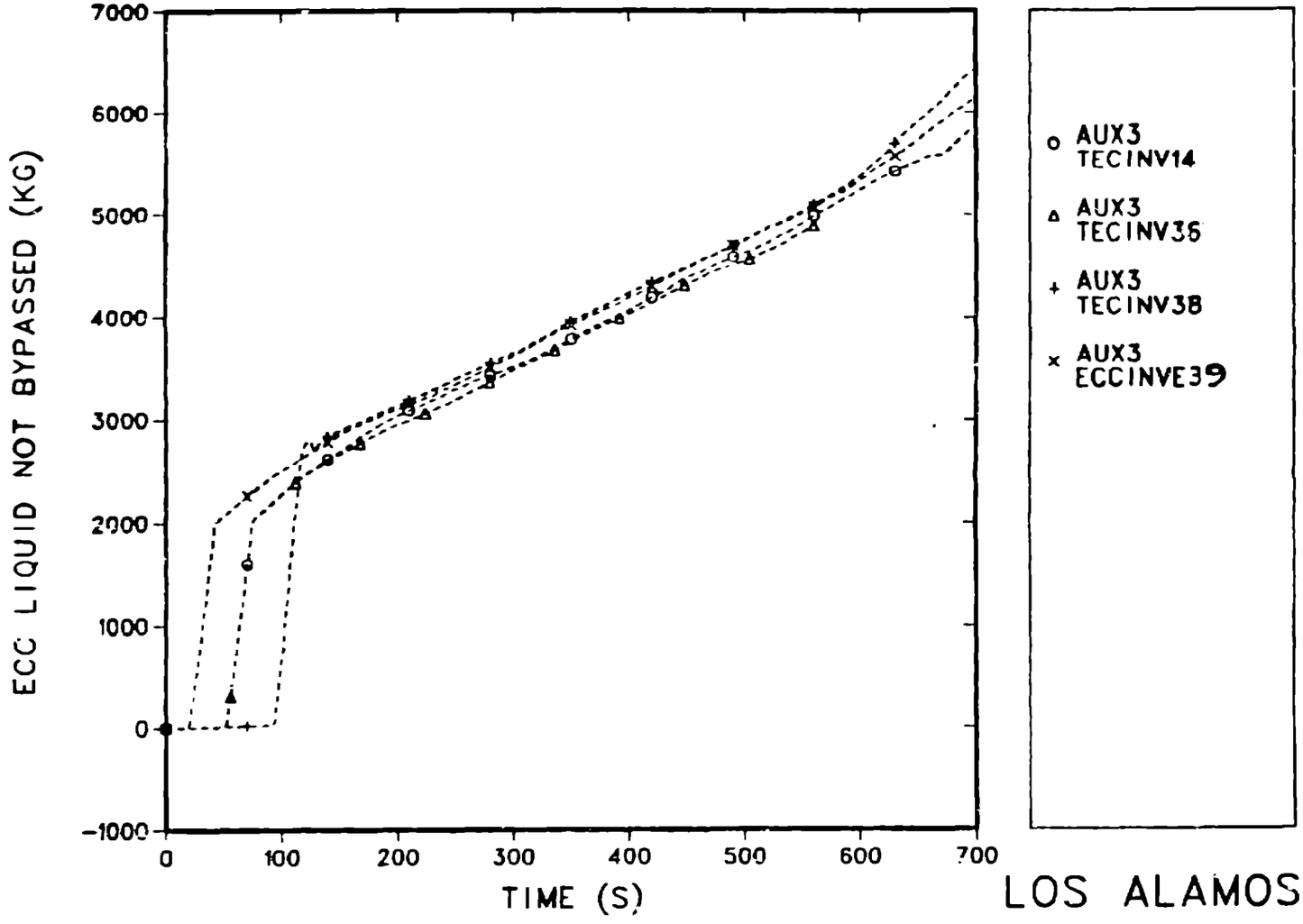


Fig. 8. ECC liquid entering the core.

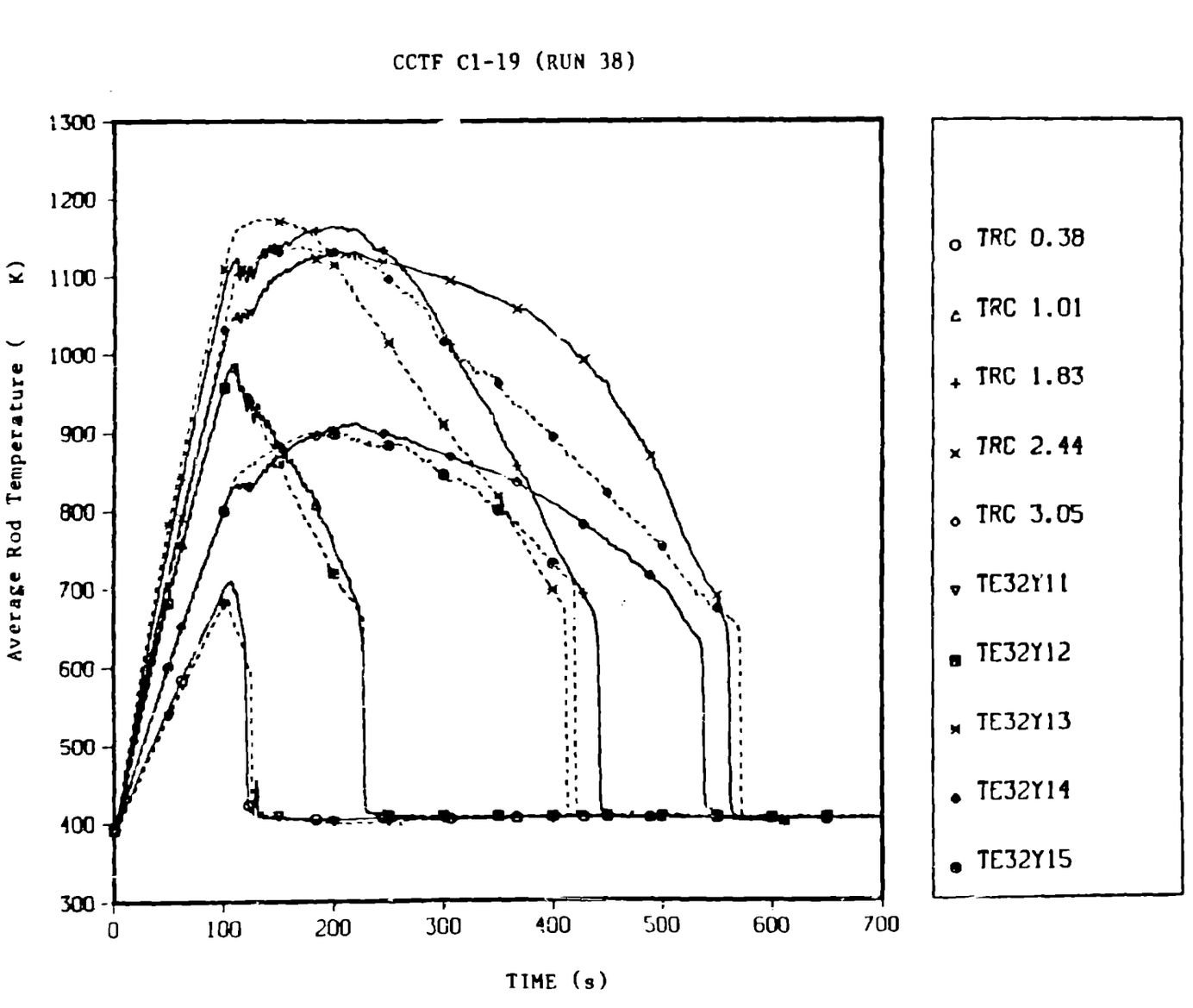


Fig. 9. Temperature response of high-power central rod.

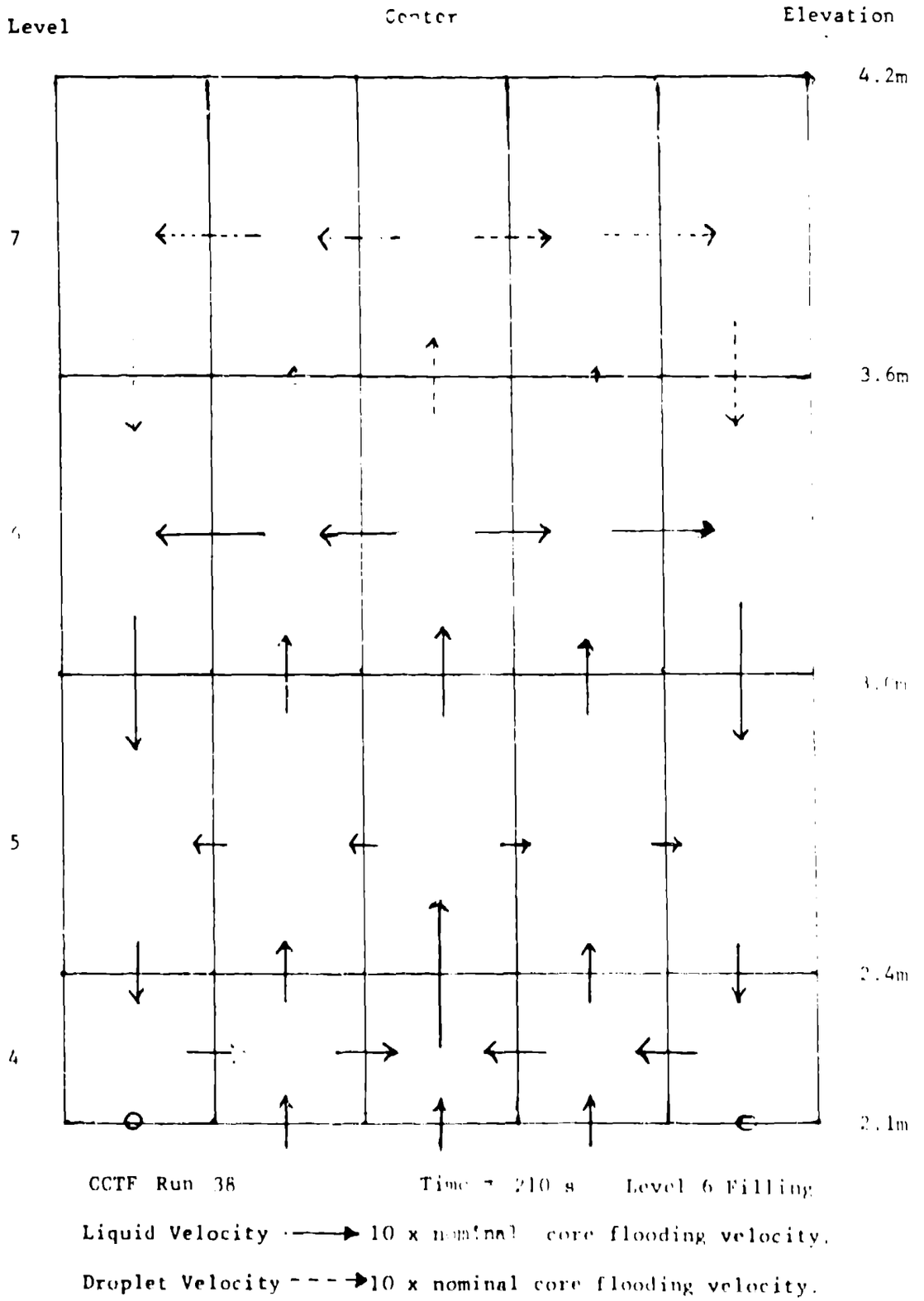


Fig. 10. Liquid velocity diagram of lower half of core for Run 38 at 210 s.

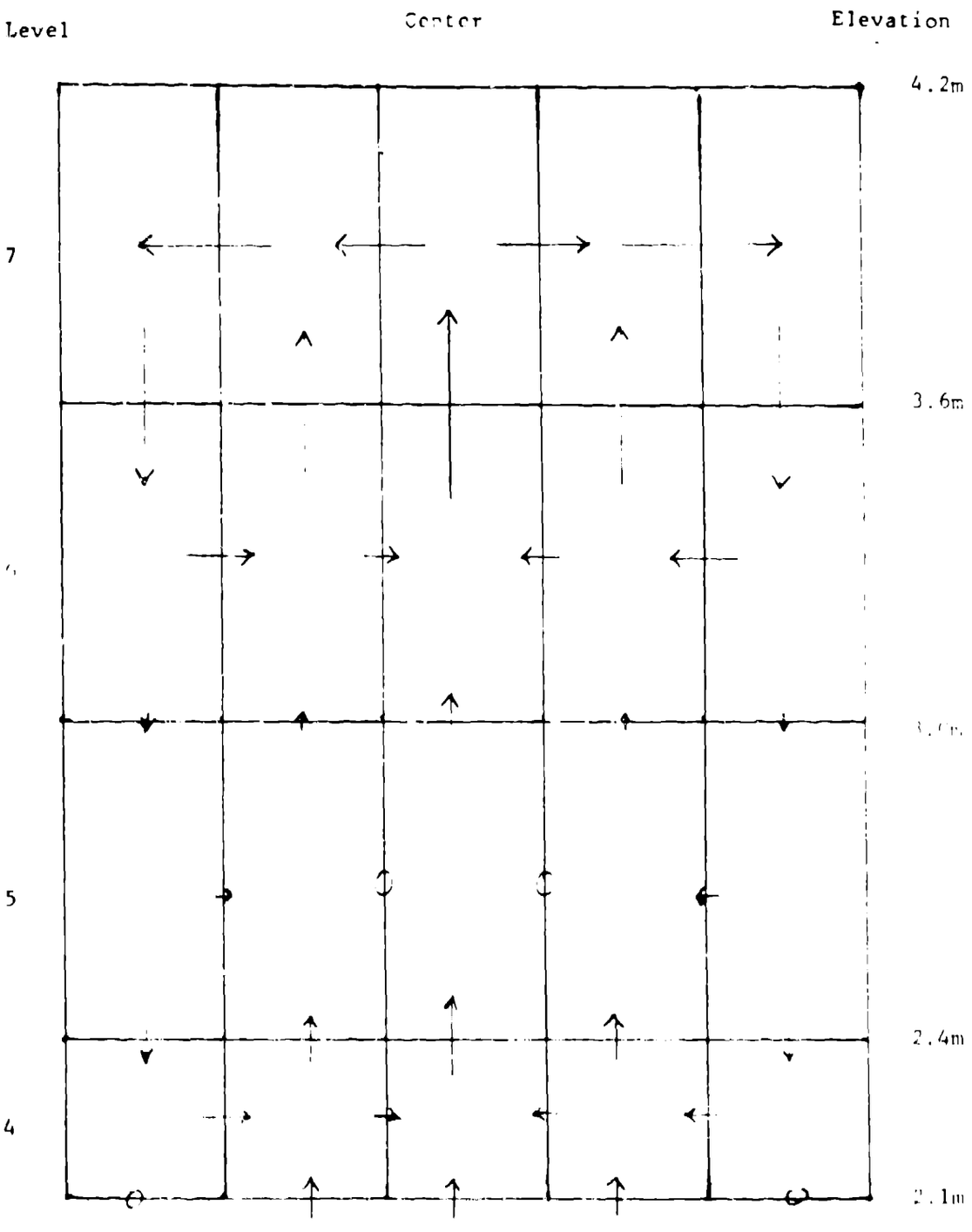


Fig. 11. Liquid velocity diagrams of lower half of core for 38 at 430 s.

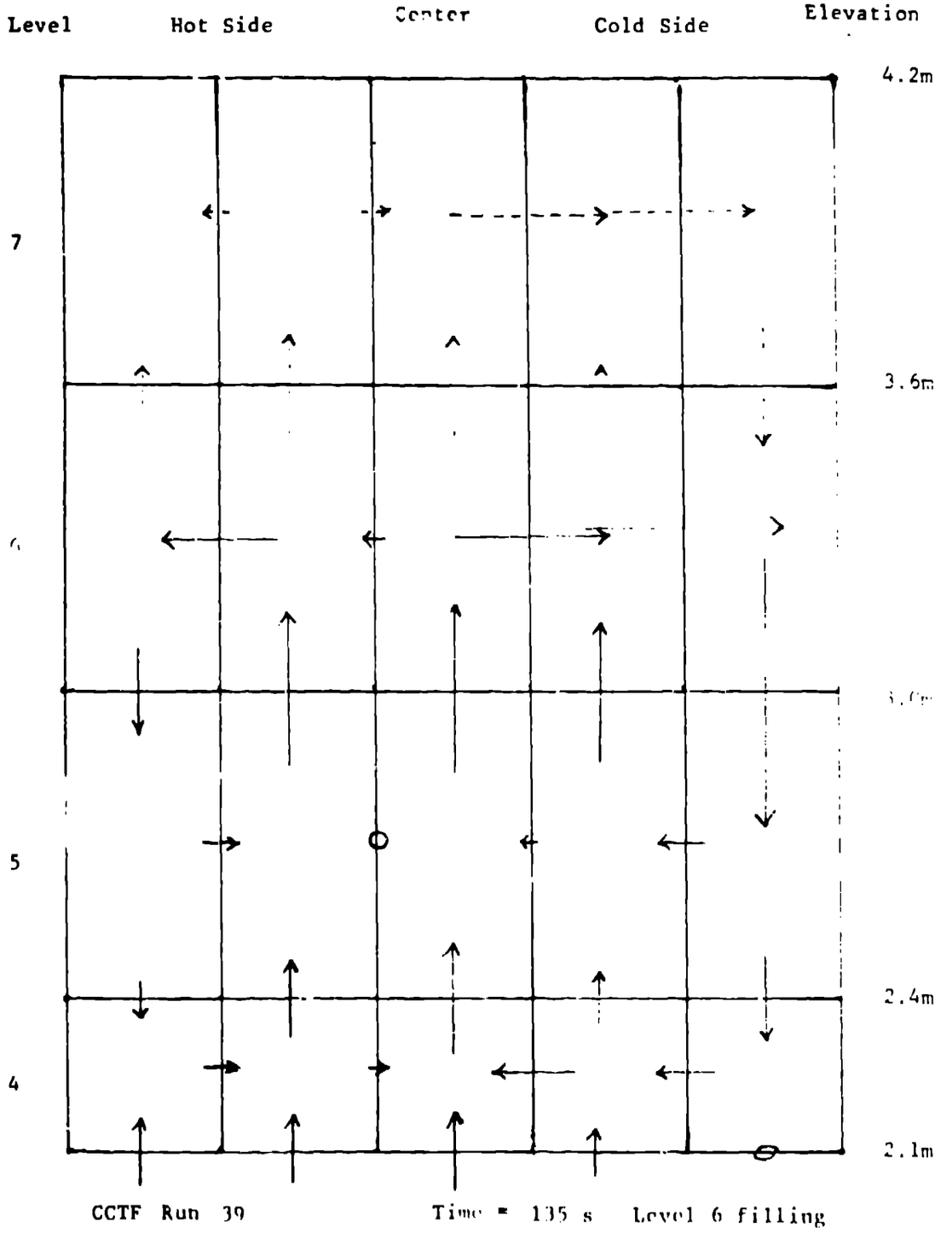


Fig. 12. Liquid velocity diagram for lower half of core for Run 39 at 135 s.

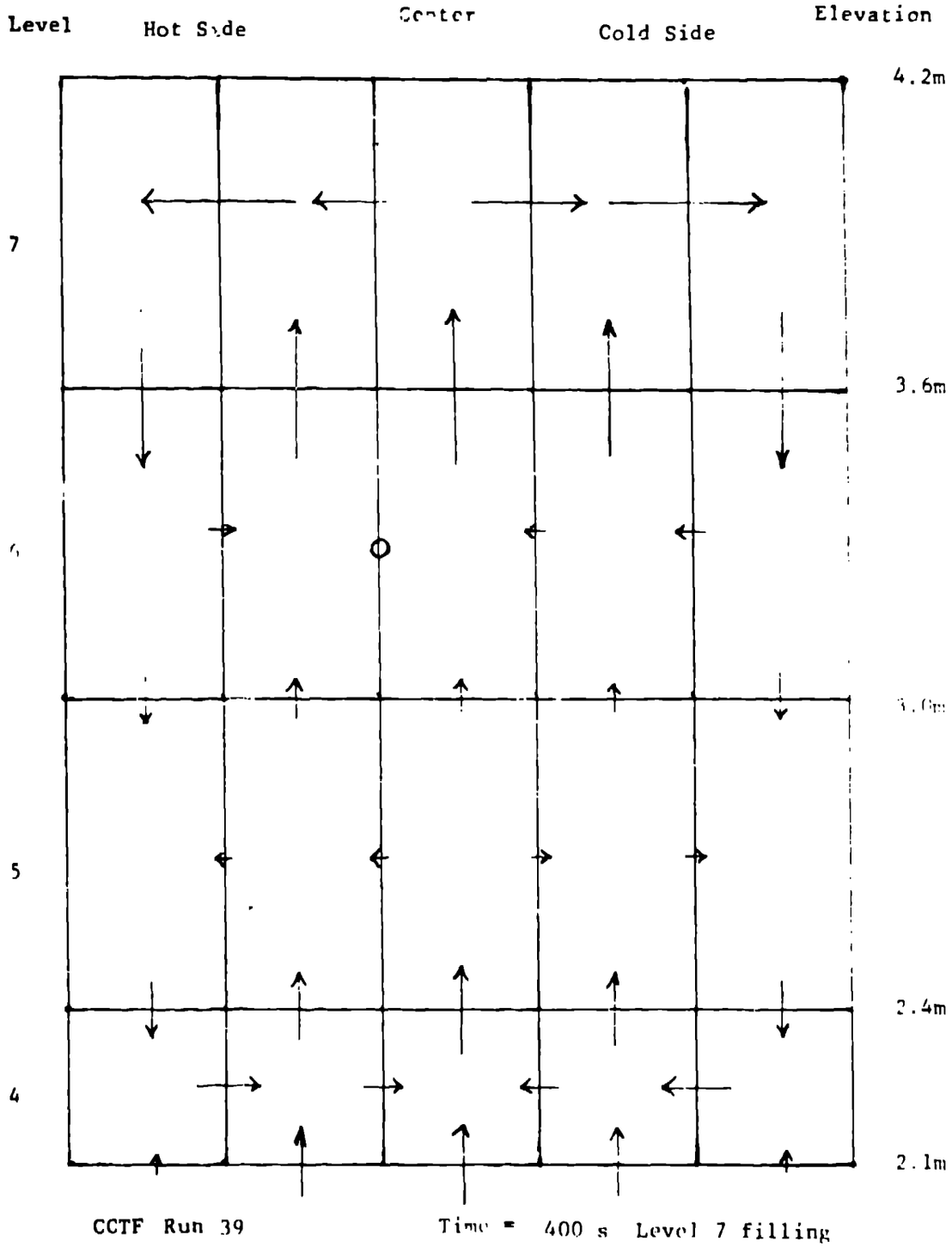


Fig. 13. Liquid velocity diagram of lower half of core for Run 39 at 430 s.